J. Braz. Chem. Soc., Vol. 22, No. 4, 660-668, 2011.
Printed in Brazil - ©2011 Sociedade Brasileira de Química
0103 - 5053 $6.00+0.00

Article

Synthesis, Characterization and Catalytic Activity of Two Novel *cis*-Dioxovanadium(V) Complexes: $[VO_2(L)]$ and $[VO_2(HLox)]$

Natália M. L. Silva,[a] Carlos B. Pinheiro,[b] Eluzir P. Chacon,[a] Jackson A. L. C. Resende,[a] José Walkimar de M. Carneiro,[a] Tatiana L. Fernández,[c] Marciela Scarpellini[c] and Mauricio Lanznaster*[,a]

[a]Instituto de Química, Universidade Federal Fluminense, Outeiro S. João Batista S/N, 24020-141 Niterói-RJ, Brazil

[b]Departamento de Física, Universidade Federal de Minas Gerais, Av. Antonio Carlos 6627, Pampulha, 31270-901 Belo Horizonte-MG, Brazil

[c]Instituto de Química, Universidade Federal do Rio de Janeiro, Av. Athos da Silveira Ramos 149, Bl. A, 21941-909 Rio de Janeiro-RJ, Brazil

Dois novos complexos $[VO_2(L)]$ e $[VO_2(HLox)]$ foram sintetizados e caracterizados por espectroscopias no IV, UV-Vis e RMN, voltametria cíclica, análise elementar e difração de raios X. A síntese do ligante inédito H_2Lox também é descrita. Os complexos **1** e **2** foram obtidos pela reação de $[VO(acac)_2]$ com os respectivos ligantes HL e H_2Lox. Alternativamente, **2** foi preparado a partir da reação de HL com $[VO(acac)_2]$ na presença de hidroxilamina, e através da reação de **1** com hidroxilamina. Dados cristalográficos mostram que **1** e **2** apresentam estruturas moleculares similares, onde o centro de vanádio(V) *cis*-dioxo encontra-se coordenado em um ambiente octaédrico distorcido formado pelos ligantes L^- e $HLox^-$, respectivamente. A atividade catalítica destes compostos foi avaliada na oxidação do cicloexano, utilizando H_2O_2 e *t*-BuOOH como oxidantes. Ambos apresentam seletividade > 70% para formação de cicloexilidroperóxido. Cálculos B3LYP/6-31G(d) foram empregados na otimização da geometria e para auxiliar na atribuição do espectro eletrônico.

Two novel complexes, $[VO_2(L)]$ (**1**) and $[VO_2(HLox)]$ (**2**), were synthesized and characterized by IV, UV-Vis and NMR spectroscopy, cyclic voltammetry, elemental analysis and X-ray diffraction. The synthesis of a new ligand, H_2Lox, is also described. Complexes **1** and **2** were obtained by the reaction of $[VO(acac)_2]$ with the ligands HL and H_2Lox, respectively. Alternatively, **2** was also obtained by the reaction of HL with $[VO(acac)_2]$ in the presence of hydroxylamine, and by the reaction of **1** with hydroxylamine. Crystallographic data show that complexes **1** and **2** have similar molecular structures, in which the *cis*-dioxovanadium(V) center is coordinated to L^- or $HLox^-$, respectively, in a distorted octahedral environment. The catalytic activity of these compounds towards cyclohexane oxidation was evaluated using H_2O_2 and *t*-BuOOH as oxidants. Both complexes presented > 70% selectivity for cyclohexylhydroperoxide formation. B3LYP/6-31G(d) calculations were used to confirm the geometry and to help assign the electronic spectra.

Keywords: oxovanadium(V), bioinspired catalysts, peroxide activation

Introduction

Vanadium coordination chemistry has received attention in recent years due to its presence in several biological systems and its applications in catalysis. The first example of vanadium-dependent enzyme are the vanadium haloperoxidases (VHPOs), isolated from the marine algae *Ascophyllum nodosum*.[1,2] Later, these enzymes were isolated from different sources such as seaweed, lichens and other algae and characterized as iodoperoxidases, bromoperoxidases and chloroperoxidases, depending on the most electronegative halogen the enzyme is capable of oxidizing.[3] These enzymes are responsible for the two-electron oxidation catalyses of chloride, bromide

*e-mail: mlanz@vm.uff.br

and iodide by hydrogen peroxide and are involved in the halogenation of a large variety of organic substrates *in vivo*.[4] The discovery of its structure initiated the investigation of vanadium complexes as functional and structural models for these enzymes.[5] Special attention was given by Pecoraro and co-workers[6] who proposed the catalytic cycle for the vanadium haloperoxidases based on the behavior of several compounds.

As oxovanadium(IV) and (V) complexes are strong Lewis acids, due to their high charge to radius ratio, they can activate peroxide reagents and then be used as catalysts in several oxidation reactions of organic compounds, such as oxidation of sulfides to sulfoxides and sulfones, alkene epoxidation and hydroxylation, aromatic, alkane and alcohol oxidations, and inorganic compounds such as halide and SO_2 oxidation.[7-13]

Among the hydrocarbon oxidation reactions, catalytic oxidation of alkanes is especially interesting because this kind of reaction leads to products which have considerable application in the pharmaceutical and plastic industry. The cyclohexane oxidation into cyclohexanol and cyclohexanone is a very important industrial reaction for the manufacture of Nylon-6 and Nylon-6,6, which is achieved with high temperature and pressure.[14,15] To obtain these oxidized products, the actual industrial process requires temperature and pressure over 150 °C and 115 psi, respectively; and only about 3-8% of overall conversion is attained.[16] Thus, the development of bioinspired catalysts, which have low activation energy and require friendly oxidants, embrace important advantages from the environmental standpoint.[16-18] In this way, a number of model complexes for vanadium containing enzymes and other vanadium complexes had their catalytic properties evaluated towards the peroxidative oxidation of alkenes and aromatic hydrocarbons.[6,19-23]

In this work, we present the synthesis and characterization of two novel vanadium(V) *cis*-dioxo complexes of general formula $[VO_2(L)]$ and $[VO_2(HLox)]$, where HL = (3-[(*bis*-pyridin-2-yl-methylamino)-methyl]-2-hydroxy-5-methyl-benzaldehyde) and H_2Lox = (3-[(*bis*-pyridin-2-yl-methylamino)-methyl]-2-hydroxy-5-methyl-benzaldehyde oxime), and preliminary reactivity studies on the catalytic oxidation of cyclohexane by these complexes employing H_2O_2 or *t*-BuOOH as oxidants.

Experimental

Materials and methods

Reagents and solvents were used without further purification. High purity (99%) cyclohexane, cyclohexanol and cyclohexanone were purchased from Merck and used as received from freshly opened bottle. In addition, their purity was checked out by gas chromatography (GC). The oxidation agents H_2O_2 (30%) and *t*-BuOOH (70%) were, respectively, purchased from Vetec and Across, and their real concentrations were determined by iodometric titrations ($[H_2O_2]$ = 11.8 mol L^{-1} and [*t*-BuOOH] = 7.5 mol L^{-1}). Microanalysis were performed using a Perkin-Elmer CHN 2400 micro analyzer at the Central Analítica do Instituto de Química, Universidade de São Paulo, SP, Brazil. UV-Visible absorption spectra were recorded from 1.0×10^{-4} mol L^{-1} dimethyl sulfoxide (HPLC grade, Tedia) solutions on a Varian Cary 50 spectrophotometer, using 1 cm optical length quartz cuvettes. IR spectra (KBr pellets) were recorded on a FT-IR Spectrum One (Perkin Elmer) spectrophotometer. ^{1}H NMR spectra were recorded on a Varian Unit Plus 300 MHz spectrometer in DMSO-d_6; chemical shifts (δ) are reported in parts per million (ppm) relative to the internal standard Me_4Si. The hydrogen signals were attributed based on the coupling constant values (*J*) and 2D COSY experiments. Cyclic voltammetry experiments were carried out in a BAS Epsilon potentiostat-galvanostat system, using a conventional electrochemical cell with three electrodes: Ag/AgCl for organic media as reference, platinum wire as auxiliary, and glassy carbon as working electrode. Electrochemical grade tetrabutylammonium hexafluorophosphate ($TBAPF_6$, Sigma Aldrich) 0.1 mol L^{-1} in DMSO (Tedia Anhydrosolv) was used as supporting electrolyte, and the whole cell was deoxygenated using ultrapure argon. Ferrocene was used as an internal reference ($E_{1/2}$ = 0.40 V *vs.* NHE).[24]

Syntheses of HL and HLox

The synthesis of HL was previously reported.[25] The ligand HLox was prepared according to Scheme 1. An ethanol solution of HL (1.25 g, 3.60 mmol), hydroxylamine hydrochloride (0.50 g, 3.60 mmol) and sodium carbonate (0.38 g, 3.60 mmol) was stirred under reflux during 24 h. The solvent was removed under vacuum, and the resulting oil was dissolved in dichloromethane and washed with water. The organic layer was dried over $MgSO_4$ and the solvent was removed under vacuum. The product was obtained as a greenish viscous oil (1.04 g, 80%); ^{1}H NMR (300 MHz, $CDCl_3$, 25°C), δ 8.53 (ddd, *J* 4.98, 1.68, 0.80 Hz, 2H, H^a), 8.40 (s, 1H, H^g), 7.65 (td, *J* 7.69, 7.69, 1.78 Hz, 2H, H^c), 7.49 (d, *J* 7.84 Hz, 2 H, H^d), 7.16 (ddd, *J* 7.47, 4.99, 1.10 Hz, 2H, H^b), 7.12 (d, *J* 1.74 Hz, 2H, H^e and H^f), 3.99 (s, 4 H, N-CH_2-py), 3.88 (s, 2 H, N-CH_2-Ar), 2.24 (s, 3H, CH_3); IR ν_{max}/cm^{-1} (KBr) 1596, 1473, 1440 ν(C=C, C=N), 1231 ν(C-O), 763 δ(C-H).

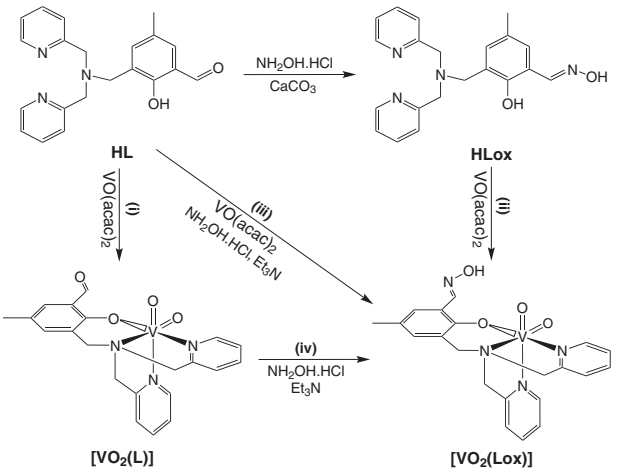

Scheme 1. Synthesis of HL, HLox, $[VO_2(L)]$ (**1**) and $[VO_2(Lox)]$ (**2**).

*Synthesis of $[VO_2(L)]$ (**1**)*

(i). To a solution of HL (174 mg, 0.5 mmol) in methanol (30 mL) was added $[VO(acac)_2]$ (132 mg, 0.5 mmol) and the mixture heated at 80 °C under stirring for 30 min. After cooling to room temperature, this solution was left undisturbed for few days, given yellow crystals that were isolated (94 mg, 43%). Found: C, 56.44; H, 4.72; N, 9.44%. Calc. for $(C_{21}H_{20}N_3O_4V)_2{\cdot}H_2O$: C, 57.54; H, 4.83; N, 9.59%. ^{1}H NMR (300 MHz, DMSO-d_6, 25°C) δ 9.22 (d, *J* 5.10 Hz, 1H, H^a), 8.65 (d, *J* 4.50 Hz, 1H, $H^{a'}$), 8.05 (td, *J* 7.50, 1.80 Hz, 1H, $H^{c'}$), 7.67 (d, *J* 7.80 Hz, 1H, $H^{d'}$), 7.56 (td, *J* 7.50, 1.80 Hz, 1H, H^c), 7.50 (t, *J* 6.60, 6.30 Hz, $H^{b'}$), 7.26-7.22 (m, 2H, H^b and H^f), 6.98 (d, *J* 2.10 Hz, 1H, H^e), 6.83 (d, *J* 7.80 Hz, H^d), 5.07 (d, *J* 12.00 Hz, 1H, CH_2-N-Ar), 4.89 (d, *J* 15.00 Hz, 1H, CH_2-N-Ar), 4.37 (d, *J* 15.00 Hz, CH_2-N-Ar), 4.06 (d, *J* 17.40 Hz, 1H, CH_2-N-Ar), 3.94 (d, *J* 12.00 Hz, CH_2-N-Ar), 3.75 (d, *J* 17.40 Hz, 1H, CH_2-N-Ar), 2.12 (s, 3H, CH_3). IR ν_{max}/cm^{-1} (KBr) ν(C=O) 1660, ν(C=C, C=N) 1610, 1568, 1471, 1456 and 1431, ν(C-O) 1262, ν(O=V=O) 895 and 875, ν(C-H) 760.

*Synthesis of $[VO_2(Lox)]$ (**2**)*

The complex $[VO_2(Lox)]$ was prepared by three different ways, according to Scheme 1, from the reaction of $[VO(acac)_2]$ and the ligand HLox (ii); of $[VO(acac)_2]$, HL and hydroxylamine (iii); and of $[VO_2(L)]$ with hydroxylamine (iv).

(ii). To a solution of HLox (90 mg, 0.25 mmol) in methanol (30 mL), $[VO(acac)_2]$ (66 mg, 0.25 mmol) was added. The mixture was heated at 80 °C under stirring for 30 min and then cooled to room temperature. Brown crystals were collected after leaving the solution resting undisturbed for few days (44 mg, 40%). Found: C, 55.63; H, 4.73; N, 12.30%. Calc. for $C_{21}H_{21}N_4O_4V$: C, 56.76; H, 4.76; N, 12.61%. ^{1}H NMR (300 MHz, DMSO-d_6, 25°C) δ 9.20 (d, *J* 5.34 Hz, 1H, H^a), 8.65 (d, *J* 5.07 Hz, 1H, $H^{a'}$), 8.00 (s, 1H, H^g), 7.97 (d, *J* 7.62 Hz, 1H, $H^{c'}$), 7.60 (d, *J* 7.85 Hz, 2H, $H^{d'}$), 7.58 (d, *J* 7.61 Hz, 2H, H^c), 7.45 (t, *J* 6.90, 6.20 Hz, 1H, $H^{b'}$), 7.23 (t, *J* 6.17, 6.10 Hz, 1H; H^b), 7.04 (d, *J* 1.91 Hz, 1H, H^f), 6.92 (d, *J* 2.07 Hz, 1H, H^e), 6.88 (d, *J* 8.05 Hz, 1H, H^d), 5.11 (d, *J* 12.14 Hz, 1H, CH_2-N-Ar), 4.83 (d, *J* 14.83 Hz, 1H, CH_2-N-Ar), 4.33 (d, *J* 14.93 Hz, 1H, CH_2-N-Ar), 4.09 (d, *J* 17.63 Hz, 1H, CH_2-N-Ar), 3.88 (d, *J* 12.18 Hz, 1H, CH_2-N-Ar), 3.75 (d, *J* 17.56 Hz, 1H, CH_2-N-Ar), 2.11 (s, 3H, CH_3); IR ν_{max}/cm^{-1} (KBr) ν(C=C, C=N) 1596, 1473 and 1440, ν(C-O) 1231, ν(O=V=O) 895 and 854, ν(C-H) 763.

(iii). To a solution of HL (174 mg, 0.50 mmol) in methanol (30 mL), $[VO(acac)_2]$ (132 mg, 0.50 mmol), hydroxylamine hydrochloride (52 mg, 0.75 mmol) and triethylamine (0.14 mL, 1.0 mmol) were added, and the mixture heated to 80 °C under stirring for 1 h and then cooled to room temperature. Brown crystals were collected after leaving the solution rest undisturbed for few days (111 mg, 50%).

(iv). To a solution of **1** (50 mg, 0.12 mmol) in methanol (30 mL), hydroxylamine hydrochloride (12 mg, 0.18 mmol) and triethylamine (34 μL, 0.24 mmol) were added, and the mixture heated to 80 °C under stirring for 1 h and then cooled to room temperature. Brown crystals were collected after leaving the solution resting undisturbed for few days.

Crystal structure determination

X-ray diffraction data collection for both complexes were performed on a Bruker-Kappa-CCD diffractometer (LdrX-UFF) using graphite-monochromatized MoKα radiation (λ = 0.71073 Å) at room temperature.[26] Final unit cell parameters were based on the refinement of randomly selected reflections positions (DIRAX programs) during PHICHI scanning.[27,28] Data integration and scaling of the reflections were performed with the EVALCCD suite.[28,29] Empirical multiscan absorption corrections using equivalent reflections were performed with the program SADABS.[30] The molecular structures were solved by direct methods using the SHELXS-97 program.[31] The positions of all atoms could be unambiguously assigned on consecutive difference Fourier maps. Refinements were performed using SHELXL-97 based on F^2 through full-matrix least square routine.[32] All but hydrogen atoms were refined with anisotropic atomic displacement parameters. Hydrogen

atoms were added geometrically in the structure and further refined according to the riding model.[33] Crystal structure and refinement data for compounds **1** and **2** are summarized in Table S1. ORTEP of the structures are depicted in Figures 3 and 4.[34] Relevant distances and angles are indicated in Table 2. Atomic coordinates and complete crystal structure results are given as supplementary material.

Theoretical calculations

Density functional calculations were carried out using the Gaussian03W molecular orbital package.[35] Geometries were fully optimized (starting from the structure obtained after the X-ray diffraction data refinements) using the B3LYP functional with the standard 6-31G(d) basis set.[26,37] NMR spectra for the optimized geometry were calculated using B3LYP/6-31G(d). Electronic spectra were calculated using the TD (time dependent) methodology available in Gaussian with the B3LYP/6-31+G(d) method.

Reactivity studies

The cyclohexane oxidation experiments followed typical procedures reported previously.[15] Reactions were carried out in acetonitrile, using either H_2O_2 or *t*-BuOOH as oxidant and the complexes **1** and **2** as catalysts. The catalyst:substrate:oxidant ratio was of 1:1000:1000, were the catalyst concentration was kept at 7×10^{-4} mol L^{-1}. The reactions were carried out under inert atmosphere (argon) at room temperature in a sealed round-bottomed flask. The catalyst was dissolved in acetonitrile, the solution was deoxygenated with argon and the oxidant was added with a syringe. Catalytic reactions were triggered by the addition of cyclohexane under stirring. After 24 h it was quenched by addition of an aqueous solution of Na_2SO_4 (0.4 mol L^{-1}) and extracted with 10 mL of diethyl ether. The organic layers were combined, dried over anhydrous Na_2SO_4 and analyzed by GC (gas chromatography). Control experiments were carried out in the same conditions in the absence of catalyst. The products were determined by separated injection of standard grade cyclohexanol and cyclohexanone, and confirmed by GC-MS. Cyclohexylhydroperoxide was identified as the product with higher retention time (14.0 min) and confirmed by GC-MS.

Results and Discussion

Syntheses

The ligand HL was prepared following a procedure reported previously, and characterized by ^{1}H NMR. The H_2Lox was obtained by a reaction between HL and hydroxylamine, as a greenish viscous oil with 80% yield. The conversion of the aldehyde of HL to the oxime in H_2Lox was confirmed by IR and ^{1}H NMR spectroscopy. The most relevant information from IR data is the presence of an intense peak at 1678 cm^{-1} in the spectrum of HL, assigned to the C=O stretching of benzaldehyde, which is absent in the spectrum of H_2Lox (Figure 1). The ^{1}H NMR spectra show that the signal of H^g in HL shifts from δ 10.43 to 8.40 ppm in the spectrum of HLox, due to the conversion of HC(R)=O into HC(R)=NOH. The full assignment of HL and HLox NMR spectra is shown in Figure 2.

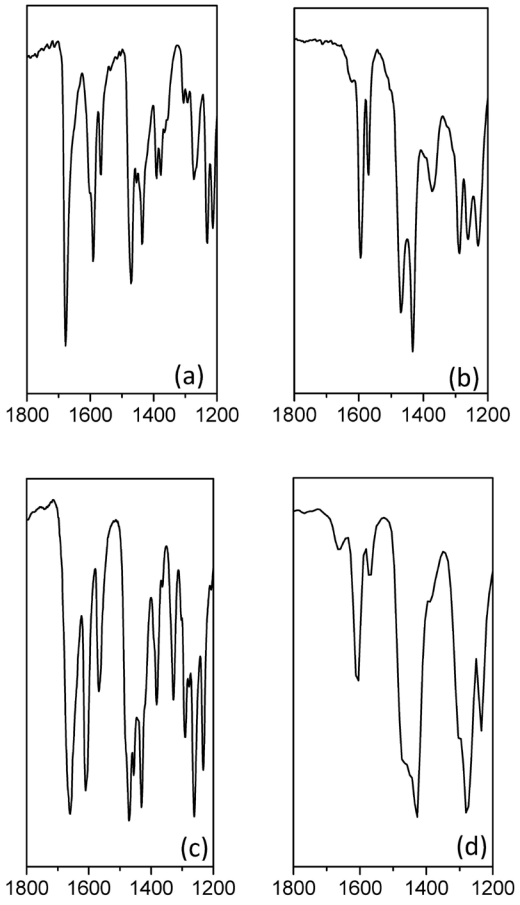

Figure 1. Selected IR spectra (KBr, transmittance / % *vs.* frequency / cm^{-1}) of HL (a), H_2Lox (b), **1** (c) and **2** (d).

The reaction of HL with $[VO(acac)_2]$ in methanol produced **1** as yellow single crystals after slow evaporation of the mother solution. Complex **2** was prepared by three different procedures, according to Scheme 1. In all cases, brown single crystals were obtained after slow evaporation of the mother solution. Besides the same color and morphology, IR and ^{1}H NMR analyses confirmed the same composition for the solids obtained from the three procedures. Figures 1 and 2 show the main spectral

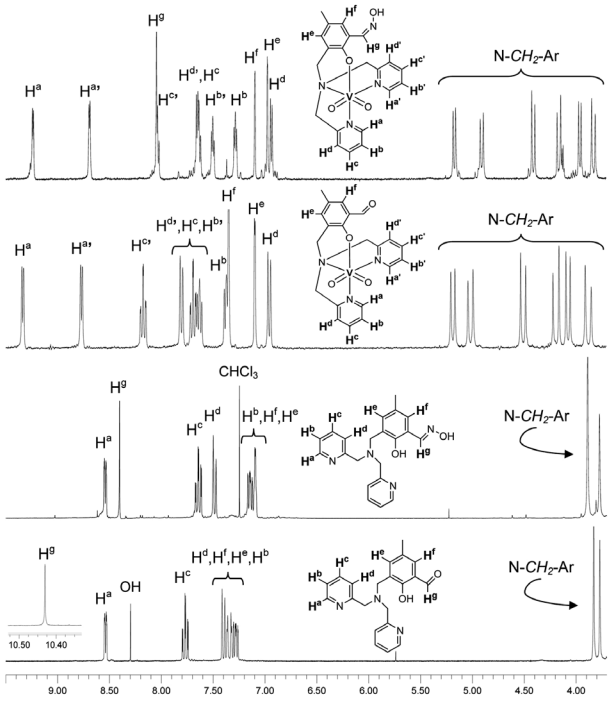

Figure 2. ^{1}H RMN spectra of HL and H_2Lox in $CDCl_3$, and of **1** and **2** in DMSO-d_6 (from the bottom to the top, respectively).

remarks for complexes **1** and **2** compared with their precursor ligands HL and HLox. Although changes in frequencies of almost all peaks were observed in IR spectra after complexation, the general feature of ligands spectra remained in their respective complexes. The most drastic change in the ligands spectra, however, was observed by ^{1}H NMR after coordination. For the free ligands, the hydrogen atoms H^a–H^d are equivalent to $H^{a'}$–$H^{d'}$, as the two pyridine rings have similar chemical environments. The same happens with the –CH_2– hydrogen atoms, observed as two singlet peaks between δ 3.5 and 4.0 ppm. For the complexes, each hydrogen atom of the ligand, aliphatic and aromatic, can be associated with an individual peak in the spectra. This fact indicates that after complexation, one single conformation of the ligand is arranged around the metal center. As electron density is transferred to the metal through the *N*,*O*-donor atoms, the chemical environment of each H atom is now different. The full assignment of the spectra shown in Figure 2 was performed according to 2D COSY experiments of all compounds and calculation of the ^{1}H NMR spectrum for complex **1**.

X-ray structures

The molecular structures of complexes **1** and **2** consist of identical distorted octahedral environments, in which the ligands L^- and Lox^-, respectively, are coordinated around the *cis*-dioxo vanadium center. The three nitrogen atoms, from the two pyridines and the tertiary amine, are arranged in a *facial* configuration, in such a way that pyridine-N1 is *trans* to phenol-O1, pyridine-N2 is *trans* to oxo-O2 and the tertiary-N3 is *trans* to oxo-O3. In both complexes, the aldehyde and oxime groups remain uncoordinated. The asymmetric unit of **1** contains two molecules of complex and one water molecule, connected by hydrogen bonds (Figure 3). The aldehyde-O4B atom of molecule B binds one of the H atoms of the water, while the other water hydrogen atom binds the oxo-O2A atom of molecule A. For complex **2**, the crystal packing is assured by intramolecular hydrogen bonds, in which the hydrogen atom of the oxime of one molecule binds the oxo-O2 atom of the next one (Figure 4). These hydrogen bonds direct the crystalline packing towards [100] direction. Table 1 summarizes the hydrogen-bonds for **1** and **2**.

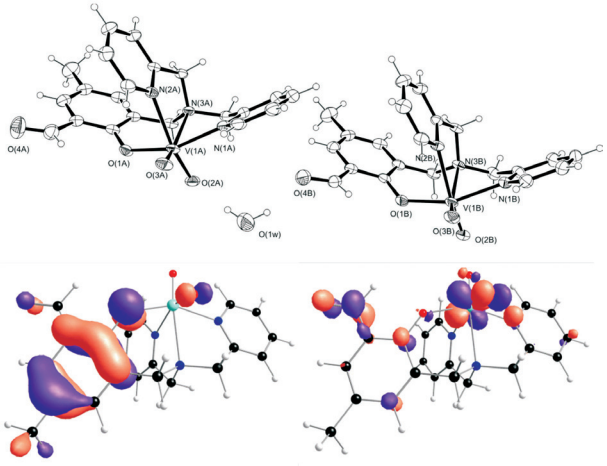

Figure 3. ORTEP[32] (top) and frontier orbitals HOMO (bottom, left) and LUMO (bottom, right) of complex **1**.

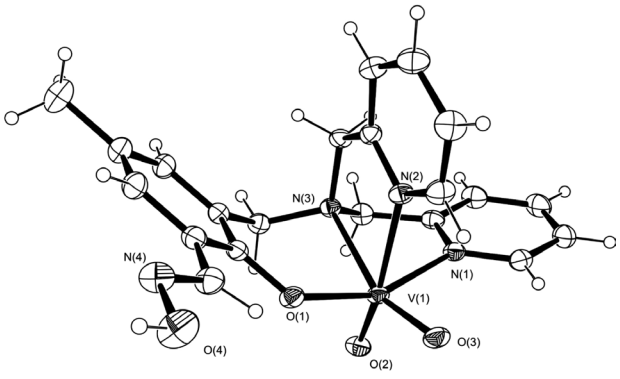

Figure 4. ORTEP[32] of complex **2**.

As can be observed in Table 2, the bond lengths and angles around the metal center are very similar for both complexes. According to information retrieved from the

Table 1. Hydrogen-bond geometry for **1** and **2** (Å, °)

D—H···*A*	*D*—H	H···*A*	*D*···*A*	*D*—H···*A*
[VO_2(L)]				
O1W—H1W2···O4B	0.86	2.06	2.864(5)	155
O1W—H1W1···O2A	0.86	1.95	2.809(5)	170
[VO_2(Lox)]				
O4—HOx···O2	0.82	2.00	2.794(3)	163

Table 2. Bond lengths (Å) and angles (°) for **1** and **2**

Complex	[VO_2(L)] (**1**)			[VO_2(Lox)] (**2**)
	Molec. A	Molec. B	B3LYP	
V1-O1	1.949(3)	1.947(3)	1.908	1.932(2)
V1-O2	1.654(3)	1.642(3)	1.609	1.668(6)
V1-O3	1.632(3)	1.639(3)	1.607	1.631(6)
V1-N1	2.150(4)	2.135(4)	2.191	2.151(2)
V1-N2	2.306(3)	2.325(3)	2.373	2.286(2)
V1-N3	2.312(3)	2.315(3)	2.421	2.304(7)
O2-V1-O3	106.97(2)	106.59(2)	108.99	105.97(9)
O1-V1-N1	156.69(1)	156.44(2)	153.46	156.85(7)
N1-V1-N3	72.79(1)	72.99(1)	71.62	72.99(7)
O3-V1-N2	89.99(1)	88.84(1)	90.26	88.65(8)
N3-V1-N2	72.31(1)	72.29(1)	70.09	73.07(7)

Cambridge Structural Database (CSD, Conquest),[38] for a vanadium *cis*-dioxo complex in an octahedral geometry, the average angle O=V=O is 105.8(9)°, and the average distance for V-$N_{pyridine}$ is 2.22(9) Å, for V-O_{phenol} is 1.94(5) Å, for V=O is 1.64(2) Å and for V-N_{amine} is 2.26(9) Å. These values are in a good agreement with those found for complexes **1** and **2** (Table 2). It should be noted, however, that in both complexes the V1-N1 bond is about 0.17 Å shorter than the V1-N2 bond, despite the fact that both are V-$N_{pyridine}$ bonds. This difference can be explained by the influence of the ligand *trans* to the pyridine nitrogen atoms. The N1 atom has one phenolic oxygen in the *trans* position, while N2 is *trans* to an oxo group. As the V=O bond is much shorter that the V-O_{phenol}, the bond distance of the ligand *trans* to the former (V-N2) is longer than the other (V-N1). These results are reinforced by the B3LYP/6-31G(d) calculations for [VO_2(L)].

Electronic spectra

UV-Visible spectra, in DMSO, show the presence of absorptions with maxima at 370 nm ($\varepsilon = 9 \times 10^3$ mol L^{-1} cm^{-1}) for **1** and 333 nm ($\varepsilon = 9 \times 10^3$ mol L^{-1} cm^{-1}) for **2**. A shoulder in 260-270 nm was also observed for both compounds. As the vanadium center is in a +5 oxidation state ($3d^0$ configuration), what is in agreement with the ^{1}H NMR spectra typical of diamagnetic species (Figure 2), ligand field transitions are not expected. Therefore, the observed bands should be related to LMCT and intra-ligand charge transfer transitions. To get a better insight into the UV-Vis spectra, the time dependent (TD) approach available in Gaussian was employed to calculate the electronic transitions for [VO_2(L)]. The calculated spectra at the B3LYP/6-31+G(d) level revealed two intense bands at 386 and 356 nm, which may be superimposed in the observed absorption maxima at 370 nm. The first band, at 386 nm, is assigned to the HOMO → LUMO transition, which correspond to a LMCT process involving a pπ orbital on the aromatic phenolate ring (the HOMO) and one empty 3d orbital on the metal (the LUMO). The second band, at 356 nm, is attributed to an intraligand transition involving the HOMO and the antibonding orbital of the carbonyl group. Frontier orbitals for **1** are depicted in Figure 3. In the region between 259 and 275 nm several bands of medium to high intensity are predicted, most of them involving contributions of several transitions, mainly LMCT. Kwiatkowski *et al.*[8] reported a series of amino/imino-phenolate oxovanadium(V) complexes with similar spectral features. For these complexes, the lowest energy bands, in the 349-404 nm range, were assigned to LMCT transitions involving the *p*π orbital of phenolate and the empty 3d orbital of the metal. The highest energy bands, observed in approximately 325 nm, were assigned to intraligand π–π* transitions.

Redox properties

Cyclic voltammograms (CV) of complexes **1** and **2**, in DMSO, show two reduction processes, as can be observed in Figure 5. All potentials are reported *versus* the ferrocene/ferrocinium (Fc/Fc^+) redox couple, used as internal reference.

The first process is an irreversible wave with peak potential at −1.89 V for **1** and −1.96 V for **2**. The second process, with half wave potentials at −2.19 V (ΔE = 0.11 V) for **1** and −2.23 V (ΔE = 0.16 V) for **2**, is better described as *quasi*-reversible. It was also observed for **1** a low intensity irreversible wave at −0.68 V, which seems to be related to the reduction peak at −1.89 V, as it does not appear when the scan direction is inverted, starting from −1.40 V (see Figure S2). This wave is absent in the CV of complex **2**, which has, however, an intense irreversible peak at +0.58 V that is not observed for **1**. Cyclic voltammograms of the ligands were also measured under similar conditions (Figure S3). While H_2Lox did not present any redox response in the negative segments of the CV, an irreversible peak at −2.14 V was observed for HL. Based on these data,

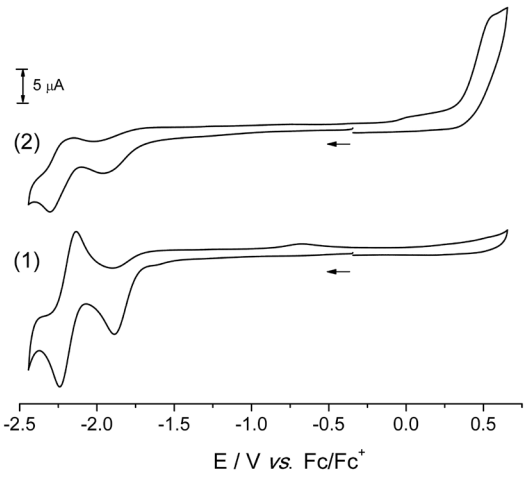

Figure 5. Cyclic voltammograms of complexes **1** (bottom) and **2** (top) in a DMSO/$TBAPF_6$ 0.1 mol L^{-1} solution, scan rate = 0.1 V s^{-1}, working electrode = glassy carbon, reference = Ag/AgCl (DMSO/$TBAPF_6$ 0.1 mol L^{-1}), auxiliary = platinum wire and ferrocene as internal reference.

the first irreversible reduction wave observed for complexes **1** and **2** is tentatively assigned to be centered in the ligand, while the more negative *quasi*-reversible reduction process is tentatively assigned to the V^{V}/V^{IV} couple. The slightly more negative reduction potentials of complex **2** could be related to the presence of the oxime group, which has a weaker electron withdrawing capability compared with the aldehyde carbonyl present in complex **1**.[39] CV experiments using dichloromethane as solvent were also carried out for **1**, with identical results to those obtained in DMSO. However, experiments in this solvent were not possible for complex **2** due to its low solubility.

Catalytic oxidation of cyclohexane

In order to investigate the potential use of complexes **1** and **2** as catalysts in oxidative processes, their reactivities were preliminary investigated through the oxidation of cyclohexane (Scheme 2). In a typical experiment, cyclohexane was oxidized in the presence of the desired complex and H_2O_2 or *t*-BuOOH. After 24 h of reaction, the products cyclohexanol (Cy-OH), cyclohexanone (Cy=O), cyclohexylhydroperoxide (Cy-OOH) and/or cyclohexyl-*t*ert-buthylhydroperoxide (Cy-OO-*t*-Bu) were detected, and the results are summarized in Table 3.

Complex **1** is the most active catalyst, presenting an overall conversion of 12% when the oxidant is H_2O_2 and only 5.7% employing *t*-BuOOH. For complex **2**, the overall conversion values are 5.7 and 2.1%, respectively, for the same oxidants. According to Table 3, the oxidation reactions exhibited better results when the oxidant was H_2O_2, probably because is a stronger oxidant than *t*-BuOOH, since their initial concentrations were kept the same to assure the

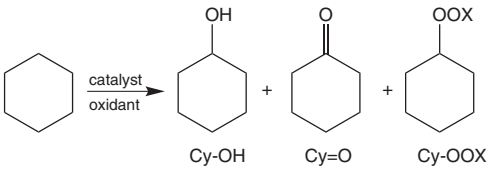

Scheme 2. Cyclohexane oxidation products (X = H or *t*-butyl).

Table 3. Product distribution for the cyclohexane oxidation after 24 h

Catalyst	Oxidant	Product	Overall conversion	Turnover	Selectivity
	H_2O_2	Cy-OH			13%
		Cy=O	12%	137	14%
1		Cy-OOH			73%
	t-BuOOH	Cy-OH			0%
		Cy=O	1.4%	15	14%
		Cy-OO-t-Bu			86%
	H_2O_2	Cy-OH			17%
		Cy=O	5.7%	62	12%
2		Cy-OOH			71%
	t-BuOOH	Cy-OH			0%
		Cy=O	2.1%	23	42%
		Cy-OO-t-Bu			58%

ratio catalyst:substrate:oxidant as 1:1000:1000. In fact, this same behavior has been observed before and may be one of the reasons of the overall conversion values using H_2O_2 to be about nine times larger compared with *t*-BuOOH, for complex **1**.[16,18,40-42] However, it cannot be excluded that acetonitrile plays an important role in this process because of a competition between the solvent and the hydrocarbon by an oxidizing species, which can be generated with both oxidants.[16,43] Although the overall conversion values for both complexes are low, they showed to be selective to the intermediates cyclohexylhydroperoxide (Cy-OOH) or cyclohexyl-*tert*-butylhydroperoxide (Cy-OO-*t*-Bu), depending if the oxidant was H_2O_2 or *t*-BuOOH. For complex **1**, the intermediate was selectively formed with yields of 73 and 86% when the oxidants were, respectively, H_2O_2 and *t*-BuOOH. For complex **2**, the yields were 73% when the oxidant was H_2O_2, and 58% when the oxidant was *t*-BuOOH. The turnover number for **1** is about twice the value observed for **2,** while both complexes present similar turnover numbers when *t*-BuOOH is used. These results are comparable with those previously reported for a $V^{IV}O$ complex in a N_3O_3 environment and for a dinuclear Cu^{II} complex.[16,18] Despite the low overall conversion presented by complexes **1** and **2**, it is higher than the corresponding uncatalyzed reactions which lead to less than 0.5% of overall conversion and selectivity to cyclohexylhydroperoxide or cyclohexyl-*tert*-butylhidroperoxide. Considering that these experiments were carried out at 1 atm pressure, room

temperature, with no co-catalysts, and that the intermediates selectively formed are easily converted to cyclohexanol, cyclohexanone and adipic acid upon reduction, which are very important to the production of Nylon-6 and Nylon-6,6, the complexes can be considered as quite efficient catalysts.

Conclusions

A novel tripodal ligand presenting an oxime pendant group (HLox) was successfully synthesized from the precursor ligand containing an aldehyde function (HL). Both HLox and HL were employed in the syntheses of two novel V^V complexes, **1** and **2**, which were also characterized as *cis*-dioxo V^V systems. It was demonstrated that complex **2** can be prepared by three different pathways: from HLox, from HL and from complex **1**. Complexes **1** and **2** presented overall conversions towards the cyclohexane oxidation between 5.7 and 12% using the friendly oxidant H_2O_2, with high selectivity (up to 85%) to the cyclohexylhydroperoxide intermediate in mild conditions (1 atm and room temperature). The overall conversion, turnover number and selectivity obtained for complexes **1** and **2** are in the range of those values found for other oxovanadium complexes previously reported.[10,16,19,22]

Supplementary Information

Crystallographic data have been deposited at the Cambridge Crystallographic Data Centre (deposition numbers CCDC 772836 (**1**) and CCDC 772836 (**2**). Copies of available material can be obtained by request to CCDC, 12 Union Road, Cambridge CB2 1EZ, UK (fax 44-1223-336033 or e-mail: deposit@ccdc.cam.ac.uk).

Acknowledgments

We thank the financial support conceived from CNPq, FAPERJ, FINEP, PIBIC-UFF, and the X-Ray Diffraction Laboratory at Universidade Federal Fluminense (LdrX-UFF) for the data collection.

References

1. Vilter, H.; *Bot. Mar.* **1983**, *26*, 451.
2. Vilter, H.; *Phytochem*. **1984**, *23*, 1387.
3. Soedjak, H. S.; Butler, A.; *Inorg. Chem.* **1990**, *29*, 5015.
4. Butler, A.; Walker, J. V.; *Chem. Rev.* **1993**, *93*, 1937.
5. Rehder, D.; *Coord. Chem. Rev.* **1999**, *182*, 297; Colpas, G. J.; Hamstra, B. J.; Kampf, J. W.; Pecoraro, V. L.; *J. Am. Chem. Soc.* **1996**, *118*, 3469; Colpas, G. J.; Hamstra, B. J.; Kampf, J. W.; Pecoraro, V. L.; *J. Am. Chem. Soc.* **1994**, *116*, 3627.
6. Hamstra, B. J.; Colpas, G. J.; Pecoraro V. L.; *Inorg. Chem.* **1998**, *37*, 949.
7. Sun, J.; Zhu, C.; Dai, Z.; Yang, M.; Pan, Y.; Hu, H.; *J. Org. Chem.* **2004**, *69*, 8500; Blum, S. A.; Bergman, R. G.; Ellman, J. A.; *J. Org. Chem*. **2003**, *68*, 150.
8. Kwiatkowski, E.; Romanowski, G.; Nowicki, W.; Kwiatkowski, M.; Suwinska, K.; *Polyhedron* **2003**, *22*, 1009.
9. Mimoun, H.; Mignard, M.; Brechot, P.; Saussine, L.; *J. Am. Chem. Soc.* **1986**, *108*, 3711.
10. Mimoun, H.; Saussine, L.; Daire, E.; Postel, M.; Fischer, J.; Weiss, R.; *J. Am. Chem. Soc.* **1983**, *105*, 3101.
11. Shulpin, G. B.; Attanasio, D.; Suber, L.; *J. Catal.* **1993**, *142*, 147; Bonchio, M.; Conte, V.; Di Furia, F.; Modena, G.; *J. Org. Chem.* **1989**, *54*, 4368; Conte, V.; Di Furia, F.; Modena, G.; *J. Org. Chem.* **1988**, *53*, 1665.
12. Secco, F.; *Inorg. Chem.* **1980**, *19*, 2722.
13. Bhattacharjee, M. N.; Chaudhuri, M. K.; Islam, N. S.; *Inorg. Chem.* **1989**, *28*, 2420.
14. Saji, P. V.; Ratnasamy, C.; Gopinathan, S.; *US pat 6,392,093B1*, **2002**.
15. Yuan, Y.; Ji, H.; Chen, Y.; Han, Y.; Song, X.; She, Y.; Zhong, R.; *Org. Process Res. Dev.* **2004**, *8*, 418.
16. Fernández, T. L.; Souza, E. T.; Visentin, L. C.; Santos, J. V.; Mangrich, A. S.; Faria, R. B.; Antunes, O. A. C.; Scarpellini, M.; *J. Inorg. Biochem.* **2009**, *103*, 474.
17. Silva, A. C.; Fernández, T. L.; Carvalho, M. F. N.; Herbst, M. H.; Bordinhão, J.; Horn Jr, A.; Wardell, J. L.; Oestreicher, E. G.; Antunes, O. A. C.; *Appl. Catal., A* **2007**, *317*, 154.
18. Martins, L. R.; Souza, E. T.; Fernández, T. L.; Souza, B.; Rachinski, S.; Pinheiro, C. B.; Faria, R. B.; Casellato, A.; Machado, S. P.; Mangrich, A. S.; Scarpellini, M.; *J. Braz. Chem. Soc.* **2010**, *21*, 1218.
19. Silva, T. F.; Luzyanin, K. V.; Kirillova, M. V.; Silva, M. F. G.; Martins, L. M. D. R. S.; Pombeiro, A. J. L.; *Adv. Synth. Catal*. **2010**, *352*, 171.
20. Kirillova, M. V.; Kuznetsov, M. L.; Romakh, V. B.; Shul'pina, L. S.; Silva, J. J. R. F.; Pombeiro, A. J. L.; Shulpin, G. B.; *J. Catal.* **2009**, *267*, 140.
21. Baran, E. J.; *J. Inorg. Biochem.* **2000**, *80*, 1.
22. Reis, P. M.; Silva, J. A. L.; Silva, J. J. R. F.; Pombeiro, A. J. L.; *Chem. Commun*. **2000**, 1845.
23. Butler, A.; Clague, M. J.; Meister, G. E.; *Chem. Rev*. **1994**, *94*, 625.
24. Gagne, R. R.; Koval, C. A.; Lisensky, G. C.; *Inorg. Chem*. **1980**, *19*, 2854.
25. Karsten, P.; Neves, A.; Bortoluzzi, A.J.; Lanznaster, M.; Drago, V.; *Inorg. Chem.* **2002,** *41*, 4624; Uozumi, S.; Furutachi, H.; Ohba, M.; Okawa, H.; Fenton, D. E.; Shindo, K.; Murata, S.; Kitko, D. J.; *Inorg. Chem.* **1998**, *37*, 6281.
26. Nonius; *COLLECT*, Nonius BV: Delft, The Netherlands, 1998.
27. Duisenberg, A. J. M.; *J. Appl. Crystallogr.* **1992**, *25,* 92.

28. Duisenberg, A. J. M.; Hooft, R. W. W.; Schreurs, A. M. M.; Kroon, J.; *J. Appl. Crystallogr.* **2000**, *33*, 893.
29. Duisenberg, A. J. M.; Kroon-Batenburg, L. M. J.; Schreurs, A. M. M.; *J. Appl. Crystallogr.* **2003**, *36*, 220.
30. Sheldrick, G. M.; *SADABS, Program for Empirical Absorption Correction of Area Detector Data*, University of Göttingen, Germany, 1996.
31. Sheldrick, G. M.; *SHELXS-97; Program for Crystal Structure Solution*, University of Göttingen: Germany, 1997.
32. Sheldrick, G. M.; *SHELXL-97; Program for Crystal Structure Refinement*, University of Göttingen: Germany, 1997.
33. Johnson, C. K. *Crystallographic Computing,* Ahmed: Copenhagen, Munksgaard, 1970, 207-219.
34. Farrugia, L. J.; *J. Appl. Crystallogr.* **1997**, *30*, 565.
35. *Gaussian 03, Revision B.02*; Frisch, M. J.; Trucks, G. W.; Schlegel, H. B.; Scuseria, G. E.; Robb, M. A.; Cheeseman, J. R.; Montgomery, J. A.; Vreen Jr., T.; Kudin, K. N.; Burat, J. C.; Millam, J. M.; Iyengar, S. S.; Tomsi, J.; Barone, V.; Mennucci, B.; Cossi, M.; Scalmani, G.; Rega, N.; Petersson, G. A.; Nakatsuji, H.; Hada, M.; Ehara, M.; Toyota, K.; Fukua, R.; Hasegawa, J.; Ishida, M.; Nakajim, T.; Honda, Y.; Kitao, O.; Nakai, H.; Klene, M.; Li, X.; Knox, J. E.; Hratchian, H. P.; Cross, J. B.; Adamo, C.; Jaramillo, J.; Gomperts, R.; Stratmann, R. E.; Yazyev, O.; Austin, A. J.; Cammi, R.; Pomelli, C.; Ochteski, J. W.; Ayala, P. Y.; Morokuma, K.; Voth, G. A.; Salvador, P.; Dannenberg, J. J.; Zakrzewski, V. G.; Dapprich, S.; Daniels, A. D.; Strain, M. C.; Faras, O.; Malick, D. K.; Rabu, A. D.; Raghavachari, K.; Foresman, J. B.; Ortiz, J. V.; Cui, Q.; Baboul, A. G.; Clifford, S.; Cioslowski, J.; Stefanov, B. B.; Liu, G.; Liashenko, A.; Piskorz, P.; Komaromi, I.; Martin, R. L.; Fox, D. J.; Keith, T.; Al-Laham, M. A.; Peng, C.; Nanayakkra, A.; Challacombe, M.; Gill, P. M. W.; Johnson, B.; Chen, W.; Wong, M. W.; Gonzalez, C.; Pople, J. A.; Gaussian, Inc., Pittsburg P. A., 2003.
36. Beck, A. D.; *J. Chem. Phys.* **1993**, *98*, 5648.
37. Hariharan, P. C.; Pople, J. A.; *Theor. Chim. Acta* **1973**, *28*, 213.
38. Allen, F. H.; *Acta Crystallogr., Sect. B: Struct. Sci.* **2002**, *58*, 380; Bruno, J.; Cole, J. C.; Edgington, P. R.; Kessler, M.; Macrae, C. F.; McCabe, P.; Pearson. J.; Taylor, R.; *Acta Crystallogr., Sect. B: Struct. Sci.***2002**, *58*, 389.
39. Lanznaster, M.; Neves, A.; Bortoluzzi, A. J.; Assumpção, A. M. C.; Vencato, I.; Machado, S. P.; Drechsel, S. M.; *Inorg. Chem.* **2006**, *45*, 1005.
40. Shul′pin, G. B.; Kozlov, Y. N.; *Org. Biomol. Chem.* **2003**, *1*, 2303.
41. Nizova, G. V.; Kozlov, Y. N.; Shulpin, G. B. *Russ. Chem. Bull., Int. Ed.* **2004**, *53*, 2330.
42. Carvalho, N. M. F.; Horn Jr., A.; Antunes, O. A. C.; *Appl. Catal., A* **2006**, *305*, 140.
43. Canhota, F. P.; Salomão, G. C.; Carvalho, N. M. F.; Antunes, O. A. C.; *Catal. Commun.* **2007**, *9*, 182.

Submitted: April 10, 2010
Published online: December 2, 2010

J. Braz. Chem. Soc., Vol. 22, No. 4, S1-S3, 2011.
Printed in Brazil - ©2011 Sociedade Brasileira de Química
0103 - 5053 $6.00+0.00

Supplementary Information

Synthesis, Characterization and Catalytic Activity of Two Novel *cis*-Dioxovanadium(V) Complexes: $[VO_2(L)]$ and $[VO_2(HLox)]$

Natália M. L. Silva,[a] Carlos B. Pinheiro,[b] Eluzir P. Chacon,[a] Jackson A. L. C. Resende,[a] José Walkimar de M. Carneiro,[a] Tatiana L. Fernández,[c] Marciela Scarpellini[c] and Mauricio Lanznaster*[,a]

[a] *Instituto de Química, Universidade Federal Fluminense, Outeiro S. João Batista S/N, 24020-141 Niterói-RJ, Brazil*

[b] *Departamento de Física, Universidade Federal de Minas Gerais, Av. Antonio Carlos 6627, Pampulha, 31270-901 Belo Horizonte-MG, Brazil*

[c] *Instituto de Química, Universidade Federal do Rio de Janeiro, Av. Athos da Silveira Ramos 149, Bl. A, 21941-909 Rio de Janeiro-RJ, Brazil*

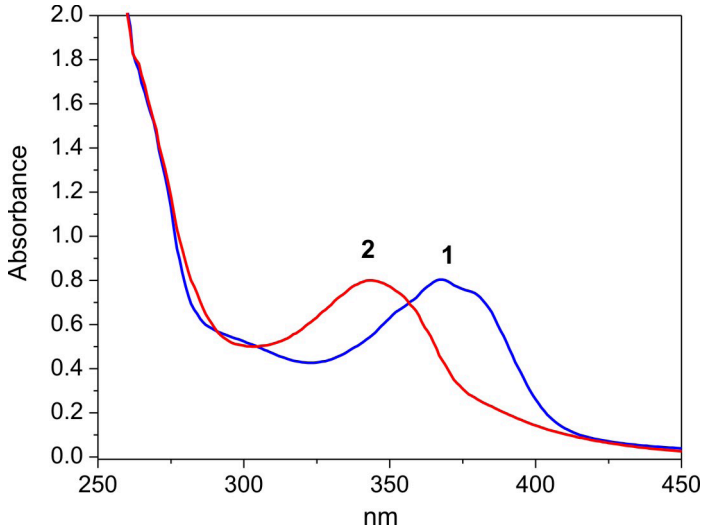

Figure S1. UV-Vis spectra for **1** and **2** recorded in DMSO solutions.

*e-mail: mlanz@vm.uff.br

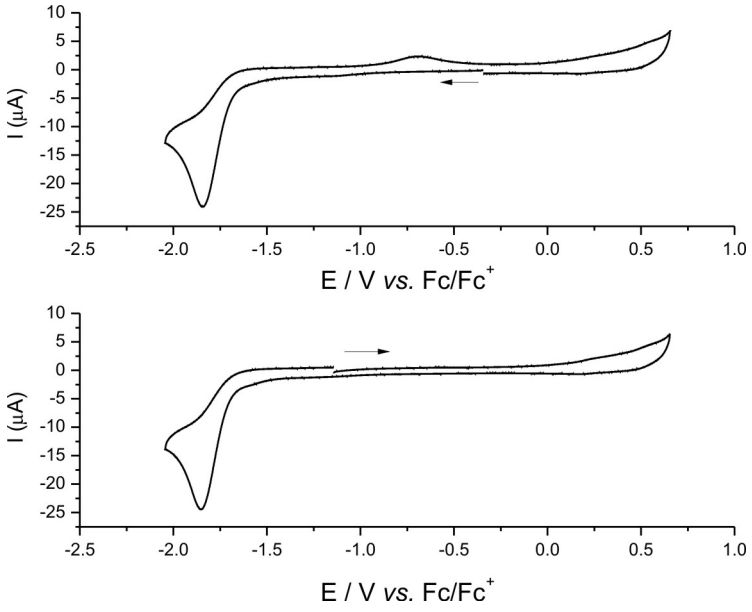

Figure S2. Cyclic voltammograms of complexes **1** in a DMSO/$TBAPF_6$ 0.1 mol L^{-1} solution, scan rate = 0.1 V s^{-1}, working electrode = glassy carbon, reference = Ag/AgCl (DMSO/$TBAPF_6$ 0.1 mol L^{-1}), auxiliary = platinum wire and ferrocene as internal reference. The arrows indicate the scan directions. This figure illustrates the dependence of the process at −0.68 V with the reduction peak at −1.89 V.

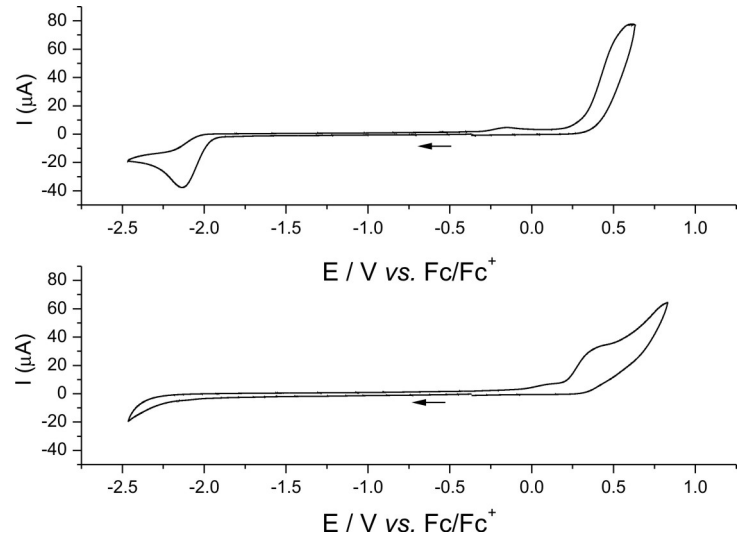

Figure S3. Cyclic voltammograms of the ligands HL (top) and H_2Lox (bottom) in a DMSO/$TBAPF_6$ 0.1 mol L^{-1} solution, scan rate = 0.1 V s^{-1}, working electrode = glassy carbon, reference = Ag/AgCl (DMSO/$TBAPF_6$ 0.1 mol L^{-1}), auxiliary = platinum wire and ferrocene as internal reference. The arrows indicate the scan direction.

Table S1. Summary of the crystal structure data collection and refinement for **1** and **2**

Identification code	$[VO_2(L)]$ (**1**)	$[VO_2(Lox)]$ (**2**)
Empirical formula	$(C_{21}H_{20}N_3O_4V)_2 \cdot H_2O$	$C_{21}H_{21}N_4O_4V$
Formula weight	876.7	444.36
Temperature	293(2) K	293(2) K
Wavelength	0.71073 Å	0.71073 Å
Crystal system	monoclinic	monoclinic
Space group	P 21/c	P21/c
Unit cell dimensions	a = 13.316(3) Å b = 14.293(3) Å c = 22.902(7) Å β = 113.70(2)°	a = 10.126(2) Å b = 15.044(3) Å c = 13.143(3) Å β = 97.61(3)°
Volume	3991.2(17) Å^3	1984.6(7) Å^3
Z	4	4
Density (calculated)	1.459 mg m^{-3}	1.487 mg m^{-3}
Absorption coefficient	0.533 mm^{-1}	0.537 mm^{-1}
F(000)	1816	920
Crystal size	0.26 × 0.25 × 0.13 mm^3	0.47 × 0.22 × 0.14 mm^3
θ range for data collection	5.16 to 25.03°	3.61 to 26.00°
Index ranges	$-15 \le h \le 15$, $-17 \le k \le 17$, $-27 \le l \le 27$	$-12 \le h \le 12$, $-18 \le k \le 17$, $-16 \le l \le 16$
Reflections collected	26034	23865
Independent reflections	6986 [$R_{(int)}$ = 0.0431]	3893 [$R_{(int)}$ = 0.0351]
Completeness to θ = 26.37°	99.1%	99.6%
Absorption correction	empirical	empirical
Max. and min. transmission	0.948 and 0.897	0.931 and 0.785
Refinement method	Full-matrix least-squares on F^2	Full-matrix least-squares on F^2
Data / restraints / parameters	6986 / 2 / 540	3893 / 0 / 271
Goodness-of-fit on F^2	1.169	1.088
Final R indices [$I > 2\sigma(I)$]	R_1 = 0.0578, wR_2 = 0.1291	R_1 = 0.0379, wR_2 = 0.0966
R indices (all data)	R_1 = 0.0872, wR_2 = 0.1386	R_1 = 0.0502, wR_2 = 0.1043
Largest diff. peak and hole	0.487 and –0.364 e.Å^{-3}	0.488 and –0.308 e.Å^{-3}